The Effect Of Electroless Sea Sand-Coated Particle On The Mechanical And Physical Properties Of Al6061/Sea Sand Composite

Hammar Ilham Akbar[1*], Ardian Dwi Saputra[2], Eko Surojo[2], Dody Ariawan[2], and Ganjar Pramudi[1]

[1] *Department of Manufacturing Engineering Technology, Vocational School, Universitas Sebelas Maret, Surakarta, 57126, Indonesia*
[2] *Department of Mechanical Engineering, Faculty of Engineering, Universitas Sebelas Maret, Universitas Sebelas Maret, Surakarta, 57126, Indonesia*
[*] *Corresponding author. E-mail: hammar_ilham@staff.uns.ac.id*

Received: Oct. 16, 2025; Accepted: Mar. 31, 2026

The use of sea sand as a reinforcing material in aluminum matrix composites (AMC) offers a promising solution for producing economical and lightweight materials. A significant challenge in this material is the low wettability of the sea sand's surface with respect to metal particles. The objectives of this research are to enhance the wettability of sea sand to enable its practical use as a reinforcement material in AMCs. The study was conducted experimentally in two stages. The first stage involved an electroless coating process. This was carried out by mixing 40 ml of nitric acid (HNO_3) with 0.5 g of aluminum (Al) powder and varying amounts of magnesium (Mg), specifically 0.1 g, 0.2 g, and 0.3 g . The coated sea sands were analyzed using scanning electron microscopy (SEM), energy dispersive X-ray spectroscopy (EDS), and X-ray diffraction (XRD). In the second stage, an aluminum 6061/sea sand composite was produced by stir casting, with the coated sea sand from the first stage as the reinforcement. The composites were then tested for density, porosity, and hardness. The results of the first-stage analysis indicate that Mg successfully modifies the surface of sea sand particles, as confirmed by SEM, EDS, and XRD tests. These tests reveal that the surface structure of sea sand becomes rough due to the presence of metal oxides. In the second-stage analysis, it was found that the Al6061/sea sand composite containing 0.1 g of Mg performed best among the variations. This variation achieves the highest values of density, porosity, and hardness at 2.643 g/cm^3, 1.84%, and 61.5 BHN , respectively.

Keywords: electroless;, sea-sand; Al6061; composite

http://dx.doi.org/10.6180/jase.202609_32.011

1. Introduction

The demand for durable and lightweight materials is increasing each year. Materials that provide high strength while maintaining a low weight can lead to significant energy savings in the automotive industry and other engineering applications [1]. One of the most advanced lightweight materials available is aluminum composite [2]. In aluminum matrix composites (AMCs), aluminum serves as the matrix material. To improve their properties, reinforcing materials are added to these composites [3]. However, the use of traditional ceramic reinforcements in AMCs, such as Al_2O_3, SiC, SiO_2, and TiO_2, can significantly increase production costs [4]. As a result, researchers are exploring various organic waste materials as alternatives to these conventional ceramic compositions. Additionally, certain ceramic and oxide compounds, including Fe_3O_4, SiO_2, and Al_2O_3, can further enhance the strength of AMCs [5].

In the last few decade, researchers have increasingly

focused on using organic and agroindustrial waste materials as reinforcement in AMC. Some examples of these materials include rice husk ash, neem seed biochar, and groundnut shell powder, as well as inorganic waste materials such as fly ash, bagasse ash, and volcanic ash. A study conducted by Jannet et al. [6] explored the use of neem seed biochar as a reinforcing material in the production of AMCs. The researchers employed the stir casting method to produce AMCs with varying reinforcement weight fractions of 0 wt%, 2.5 wt%, 5 wt%, and 7.5 wt%. The results indicated that the AMC containing 7.5% neem seed biochar demonstrated the best performance, showing an 18% increase in tensile strength compared to the unreinforced material [6]. Another literature review conducted by Yadav et al. [7] explored the use of rice husk as a reinforcement material in AMC with various aluminium matrix alloys. adding rice husk could enhance the micro-hardness of the AMC depending on the specific fraction of reinforcement used [7]. Additionally, research by Zhengwuvi et al. [8] investigated the use of groundnut shell ash as a reinforcement in AMC. This study found that the hardness properties decreased by up to 11.86% compared to pure Al6066 aluminum [8]. Furthermore, Panwar et al. [9] examined the incorporation of fly ash as a reinforcement material in AMC, testing weight fractions of 0 wt%, 2 wt%, and 4 wt%. The findings revealed that the hardness value of the AMC increased linearly with the addition of fly ash, reaching the highest hardness value of 89 Rockwell Hardness Number (RHN) at a composition of 4 wt% [9]. Based on the results, using organic and waste-based materials as reinforcement in AMCs generally improves the mechanical properties of the material. This improvement occurs because the reinforcement particles act as a load-bearing phase, effectively transferring and distributing stress from the aluminum matrix to the stiffer reinforcement. As a result, the occurrence of deformation and dislocation movement within the matrix can be minimized. Additionally, the presence of reinforcement enhances load transfer efficiency, which delays the initiation and propagation of cracks. Finding alternative reinforcement materials is crucial for creating affordable AMCs.

In the production of aluminum matrix composites, stir casting is the most commonly used technique due to its low cost, ease of use, and ability to create large and complex parts [10]. However, a significant challenge in manufacturing composite materials through stir casting is achieving good wettability of the reinforcement. Poor wettability can lead to a non-uniform distribution of reinforcement particles, ultimately reducing the material's overall strength and performance [11]. One effective method for improving wettability is electroless coating. This treatment enhances the bonding between the matrix and the reinforcement. In this context, bonding refers to the formation of a strong interface between the reinforcement and the matrix, which is crucial for evenly distributing the load and preventing failure. Prior research has explored the effects of the electroless coating method on the treatment of Al_2O_3 particles combined with additional Mg powder [12]. This study concludes that a combination of 0.004 moles of Mg powder and 0.018 moles of Al produces a thin layer of $MgAl_2O_4$ spinel phase. This layered structure results in improved wettability and superior mechanical properties compared to the base material. A similar phenomenon has been observed in the treatment of SiC. These modifications focus on the formation of MgO and $MgAl_2O_4$ spinel phases as crucial factors for enhancing mechanical properties. Additionally, a study conducted by Zulfia [13] identified an optimal formulation with 0.02 wt% Mg powder, which resulted in a higher modulus of elasticity.

Based on various literature studies, the development of aluminium matrix composites (AMCs) using readily available, low-cost organic and inorganic reinforcement materials from the surrounding environment shows significant potential for the future. This research aims to produce AMC material using Al6061 as the matrix and sea sand as the reinforcement. The use of sea sand is beneficial because it is economically and readily available from natural sources. Additionally, it contains SiO_2, which provides high hardness, excellent wear resistance, and good thermal stability. The primary focus is on applying an electroless coating technique for sea sand particles to increase their wettability and enhance the bond between the reinforcement and the matrix. Additionally, this research provides material characterization for coated sea-sand and mechanical testing to assess the impact of the electroless coating process on the mechanical properties of the resulting AMC material.

2. Material and methods

This research utilizes Aluminium 6061 as the composite matrix, with sea sand particles serving as the reinforcement material. The matrix material has a density of 2.7 g/cm^3. The sea sand used in this study was sourced from Samas, Yogyakarta, Indonesia, and contains other minerals, as presented in Table 1. Additionally, this research also incorporates several additional materials, including Mg powder, Al fine powder, and HNO_3.Mg powder used has a particle size between 0.06-0.3 mm with specifications Assay (complexometric) $\geq$ 98.5%, substances insoluble in $\leq$ 0.05%, and Fe (Iron) $\leq$ 500ppm. The Al fine powder used has a

Table 1. The mineral content of sea sand

Compound	Diopside	SiO_2 (Quartz)	Fe_2MgO_4 (Magnesioferrite)	Fe_3O_4 (Iron Oxide)
%	38,9	42,2	14,1	4,7

specification of Assay (complexometric) $\geq$ 90.0%, Heavy metals (as Pb) $\leq$ 0.03%, Arsenic (As) $\leq$ 0.0005%, and Iron(Fe) $\leq$ 1.0%. Finally, the purity content of HNO_3 used was 68%.

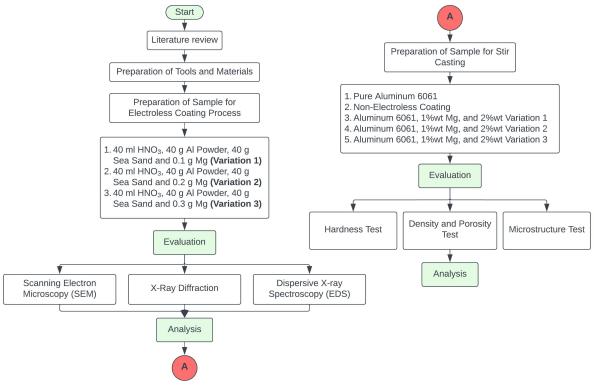

Fig. 1. Flow Chart

This research was conducted experimentally in two main steps. Fig. 1 presents complete information for the research flow diagram. The first step involved coating the sea sand, which was performed using the electroless coating method. This method aims to enhance the wettability of the surface of sea sand particles, which makes it easier to bond with other metal particles or the metal matrix material. Firstly, Sea sand was dried and cleaned with alcohol to remove contaminants. Then, the 40 ml of HNO_3 and 40 g of sea sand were placed in a container and heated to 70 °C for 30 minutes. After this initial heating, 0.5 g of aluminum fine powder and Mg powder were added to the container. The amount of magnesium powder was varied in three different quantities: 0.1 g, 0.2 g, and 0.3 g. All the material was mixed with a magnetic hot stirrer for 40 minutes at 100 °C until it was homogenously mixed. Stirring treatment under these conditions serves to remove gas bubbles and achieve an even distribution of metal oxide. The process is then continued by placing the mixed material into a furnace at 200 °C for 120 minutes. After this initial heating, the temperature is increased to 400 °C for an additional 120 minutes to facilitate oxidation. Once the heating is complete, the material is cooled to room temperature. The coated sea sand is then analyzed using SEM, XRD, and EDS. These analyses evaluate the morphological structure, crystal structure, and phase of the material, as well as the elemental composition of the samples being tested. SEM and EDS tests were conducted using a Zeiss EuO 10 machine, while XRD testing was done with a Shimadzu XRD-7000 machine (Shimadzu Corporation, Kyoto, Japan). All the preparation and characterization tests were repeated on samples with varying amounts of Mg , including 0.1 g, 0.2 g, and 0.3 g. Table 2 provides details of the variation treatments applied to the samples during the electroless coating process. Fig. 2 illustrates the appearance of sea sand before and after the coating treatment.

(a) before electroless coating

(b) after electroless coating

Fig. 2. Sea sand

The second process in this research was the manufacturing of AMC composite materials to create testing samples using the stir casting method. Aluminum 6061 was melted in a graphite crucible within a stir casting machine (see Fig. 2). The melting process was conducted at a temperature range of 720 °C to 750 °C for approximately four hours. The stir casting process commenced only after the aluminum had fully melted. The reinforcement material,

Table 2. The mineral content of sea sand

Solution	HNO_3 (ml)	Magnesium (g)	Al Powder (g)	Pasir Pantai (g)
1	40	0.1	0.5	40
2	40	0.2	0.5	40
3	40	0.3	0.5	40

derived from electroless coating, was added once the stirring began. The stirring process lasted for 10 minutes at a speed of 600 rpm . Details of the treatment variations used in the stir casting process are provided in Table 3, where each variation includes an addition of 1 % wt Mg material. The liquid AMC composite material mixture was then poured into a steel mold with dimensions of $132 \times 132 \times 40$ mm, until the sample reached a thickness of 9 mm . The mould underwent a heat treatment by being placed in a furnace at 500 °C. Once the composite mixture cooled and hardened, the following steps involved conducting hardness, density, and porosity tests, as well as a microstructure analysis. The hardness test was done using the Brinell method in accordance with the ASTM E10 standard. This test was conducted at 6 to 7 different points, utilizing a 5 mm diameter steel ball indenter with a loading of 125 kg and a pressing time of 30 seconds. In the microstructure analysis, the testing was conducted according to the ASTM E407 standard, which involves the use of Keller's Reagent as the etching solution. This reagent consists of 2 mL of hydrofluoric acid (HF), 3 mL of hydrochloric acid (HCl), 5 mL of HNO_3, and 190 mL of aquades. The sample surface was polished using progressively finer grades of sandpaper, up to approximately 2000 grid, before the test began. The specimen was then immersed in the etching solution for 20 to 25 seconds. After the etching process, the surface was rinsed with running water and examined using a Union Japan 2900 optical microscope (Tokyo, 1995). The density and porosity tests were performed to compare the actual density of the composite material with its theoretical density. The porosity was established by calculating the difference between these two densities. The actual density was measured using Archimedes' law (see Eq. (1)), while the theoretical density was calculated using the rule of mixtures (see Eq. (2)).

$$\rho_a = \frac{m_s}{m_s - m_g} \times \rho_{H_2O} \tag{1}$$

$$\rho_{\text{th}} = (\rho_{\text{matrix}} \times V_{\text{matrix}}) + (\rho_{\text{reinforcement}} \times V_{\text{reinforcement}}) \tag{2}$$

Therfore, the value of porosity can be claculated using Eq. (3).

$$\%P = 1 - \frac{\rho}{\rho_{th}} \times 100\% \tag{3}$$

Since $\rho_a, \rho_{th}, m_g, m_s, V$, and P were actual density, theoritical density, specimen wet mass, specimen dry mass, volume fraction, and porosity percentage. Dry mass is determined by weighing the specimen using a digital scale. Wet mass is obtained by weighing the specimen while it is submerged in water within a container. When the mixture consists of two or more materials, such as Al 6061, beach sand, and Mg, the materials can be combined by comparing their volume fractions and mass fractions. Using mass fractions simplifies calculations according to the rule of mixtures, as outlined in Eq. (2), where the density of the composite serves as the constant for comparison.

Fig. 3 depicts a stir casting machine. This machine uses an electric motor as its primary drive to stir the casting chamber. The casting chamber is made from a graphite crucible, which has a melting temperature of 3850 °C and a boiling temperature of 4200 °C. The crucible has a thickness of 15 mm, a diameter of 90 mm, and a depth of 115 mm. The electric drive motor is connected to the stirrer using a pulley-belt mechanism. The stirrer features four blades that are inclined at a 45 ° angle, with an outer diameter of 50 mm and an arm length of 165 mm. This component is made from stainless steel and is covered with a layer of 200 μ m of TiO_2.

3. Result and discussion

3.1. Coating of sea sand particles

The color of the sea sand particles has changed after they were coated with an electroless coating. The color change indicates that the coating process is progressing successfully. A higher concentration of magnesium produces a darker color [14]. The surface of the sea sand particles creates a new phase by forming a thin metal oxide layer. This layer acts as a binder between the matrix and the reinforcement in the AMC. The reactions involved in this process are presented in Reaction 1 (Eq. (4)) and Reaction 2 (Eq. (5)) [12].

$$HNO_3 + H_2O \longrightarrow H_3O^+ + NO_3^- \tag{4}$$

$$Mg + Al + 2H_3O^+ + NO_3^- \longrightarrow Mg^{2+} + Al^{3+} + NO_3^- + 2H_2O + H_2 \tag{5}$$

Table 3. Stir casting treatments

Reinforcement	Sea Sand (%wt)	Mg Powder (%wt)	Al6061 (%wt)
Pure Al6061	0	0	100
Non electroless coating sea sand	2	1	97
Electroless coating sea sand (0.1 g Mg)	2	1	97
Electroless coating sea sand (0.2 g Mg)	2	1	97
Electroless coating sea sand (0.3 g Mg)	2	1	97

Fig. 3. Stir Casting Machine

The reactions described in Eqs. (1) and (2) take place during the electroless coating process. This process involves heating to evaporate the H_2 produced by the previous reaction. As a result, an electrolyte containing Mg^{2+} and Al^{3+} ions is formed, and these ions move freely. The electroless process continues by mixing sea sand, which contains residual NO^-, with the previously obtained electrolyte. This mixing generates electrostatic forces between the Mg^{2+} and Al^{3+} ions and NO^- from the sea sand. These reactions lead to the formation of deposited sand, which is then dried in a furnace at 200 °C. The drying process aims to remove any remaining nitrate ions from the compound. In the subsequent phase, the furnace temperature is raised to 400 °C to facilitate the formation of the $MgAl_2O_4$ phase, as indicated in Reaction 3 (Eq. (6)). This $MgAl_2O_4$ phase formation is also clearly elaborated by previous research conducted by Zulfia and Adyatma [12]. Its metal oxide layer has enhanced the bonding characteristics between the sand and the Al6061 matrix.

$$Mg^{2+} + 2Al^{3+} + 2O_2 \longrightarrow MgAl_2O_4 \tag{6}$$

3.2. Sea sand particle characterization

The electroless coating process creates a surface on sea sand particles that appears more granular and uneven than on uncoated particles (see Fig. 3). The deposition of metal oxide material onto these particles' surfaces results in a texture that is significantly more abrasive.

This SEM analysis is conducted to evaluate the distribution and morphological structure of the sample. This analysis focuses on coated and uncoated sea sand particles, and the results are clearly presented in Fig. 4 (zoom in 10 μ m). According to the SEM analysis, it can be seen that electroless can form a newly formed metal oxide layer on the sea sand surface (see red arrow in Figs. 4b to 4d), especially with 0.1 g, 0.2 g, and 0.3 g of electroless coating. There are different surface structures between uncoated sea sand (Fig. 4a) and coated sea sand (Figs. 4b to 4d), where the coated sea sand surface produces a rougher surface structure. In Fig. 4b, it is evident that the newly formed metal oxide layer is more evenly distributed at a Mg concentration of 0.1 g. In contrast, Figs. 4c and 4d illustrate a thicker layer. As the magnesium content increases, there is a greater deposition of spinel or metal oxide, which roughens the surface of the particles. This process also leads to the formation of microcracks (middle read arrow in Figs. 4c and 4d) on the particle surface that are not wetted by the aluminum matrix. To evaluate the elemental composition and the distribution of Mg on the sea sand surface, an EDS analysis is conducted accordingly. According to surface measurements, a higher concentration during electroless coating can increase the amount of phase deposition on the surface particle. This statement is strengthened by the data presented in Table 4. The excessive deposition was resulting in a rougher surface structure. A rough surfaces result in imperfect interfacial bonding, making it difficult for the liquid metal to disperse properly. As a result, these generate a microporosity which reduces the mechanical properties of the composite.

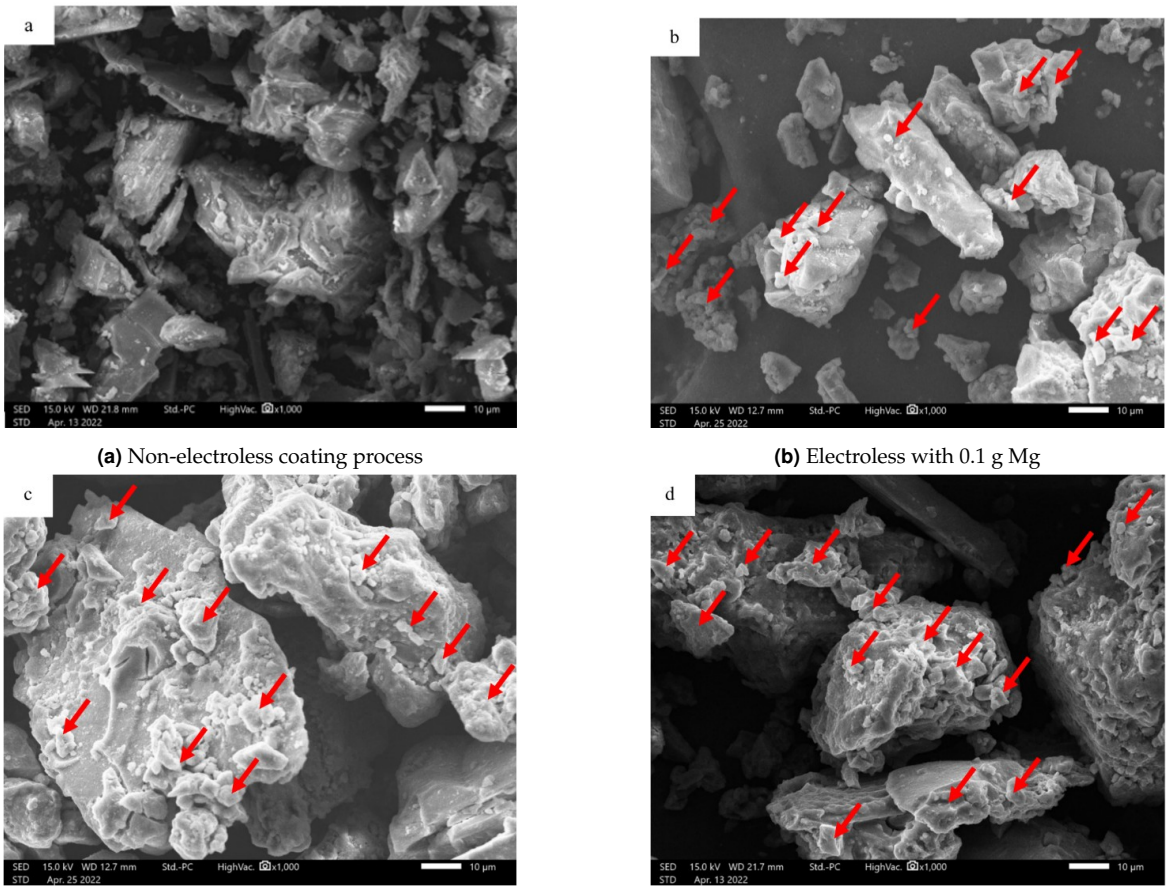

(a) Non-electroless coating process

(b) Electroless with 0.1 g Mg

(c) Electroless with 0.2 g Mg

(d) Electroless with 0.3 g

Fig. 4. The result of SEM testing on sea sand particles with (a) Non-electroless coating process, (b) Electroless with 0.1 g Mg, (c) Electroless with 0.2 g Mg, (d) Electroless with 0.3 g

Table 4. Surface area of sea sand particle

Variation	EC 0.1 g	EC 0.2 g	EC 0.3 g
Surface Area (m^2/g)	1.498	2.117	13.639

Fig. 5 presents the results of the EDS analysis for both non-electroless and electrolesscoated sea sand. The results indicate that coatings with higher Mg concentrations have a rougher and more uneven surface, resulting in the formation of metal oxide agglomerations (see Fig. 5d). The EDS test results reveal that the elemental Mg content in non-electroless-coated sea sand is 0.42%. In contrast, sea sand particles coated with electroless methods, featuring 0.1 g, 0.2 g, and 0.3 g of Mg , contain 4.59 %, 8.86 %, and 9.37 % Mg, respectively. This marks a significant increase in Mg content compared to sea sand without electroless coating. The highest Mg elemental concentration is 9.37%, with a variation of 0.3 g Mg. Moreover, the highest variation in elemental O content was observed at 74.18% for 0.1 g of Mg. The presence of O on the surface of sea sand particles enables oxidation, leading to the formation of $MgAl_2O_4$ [13]. To further investigate this, XRD testing was conducted. The formation of $MgAl_2O_4$ in aluminum composites enhances the wettability between the reinforcements.

This analysis aims to identify the crystalline phase formed on the sea sand surface after electroless coating. According to the XRD analysis, $MgAl_2O_4$ compounds are formed as indicated by the data in Fig. 6. In electroless with 0.1 g Mg, it yields peak intensities for the $MgAl_2O_4$ phase at 36.99° and 67.23°. The presence of $MgAl_2O_4$ can enhance the wettability between the reinforcement particles and the Al6061 matrix [15]. A study by Sreekumar et al. [16] indicated that the electroless coating process forms a $MgAl_2O_4$ layer on the surface of reinforcement particles, thereby improving wettability with the matrix. Additionally, the spinel phase forms on the surface of sea sand, but the intensity of the $MgAl_2O_4$ phase is crucial for determining how well the sea sand surface binds to the matrix [13].

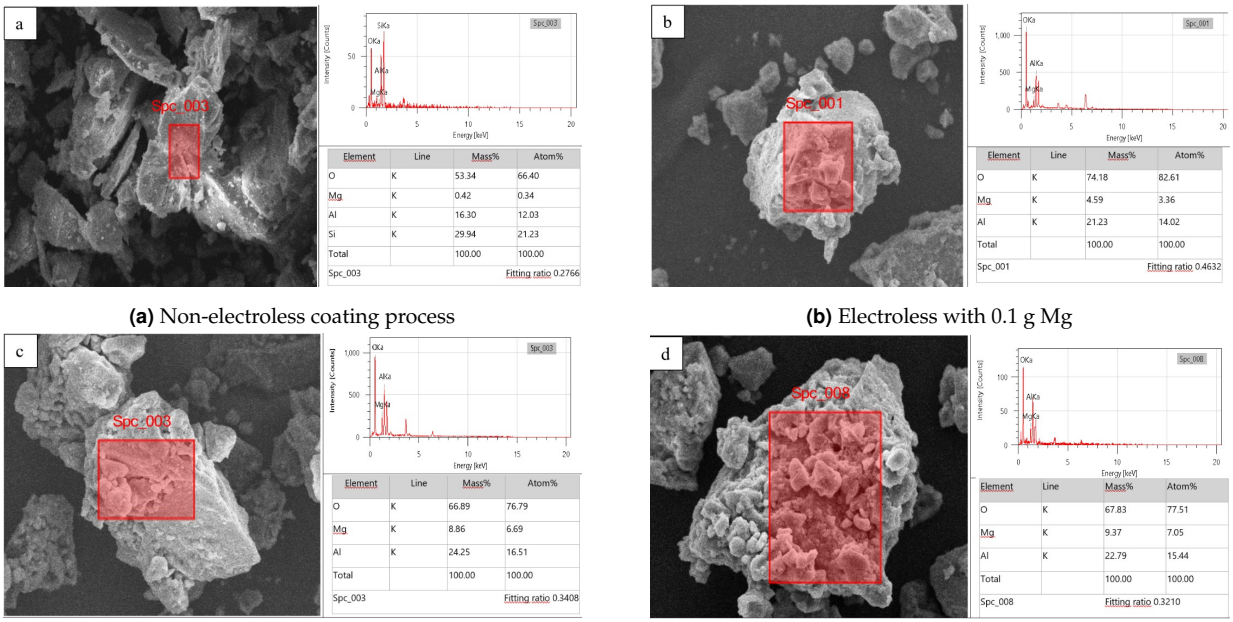

(a) Non-electroless coating process

(b) Electroless with 0.1 g Mg

(c) Electroless with 0.2 g Mg

(d) Electroless with 0.3 g Mg

Fig. 5. The result of EDS testing on sea sand particles with (a) Non-electroless coating process, (b) Electroless with 0.1 g Mg, (c) Electroless with 0.2 g Mg, (d) Electroless with 0.3 g Mg

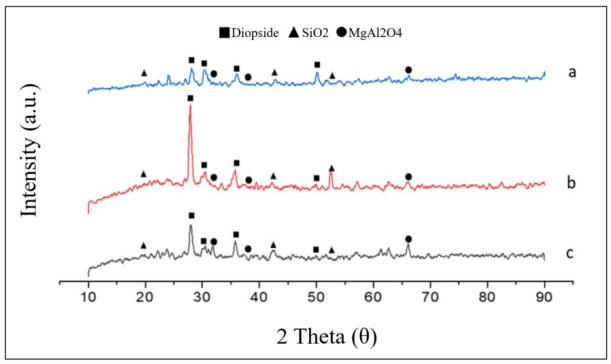

Fig. 6. XRD test results for coated sea sand: (a) 0.3 g Mg variation, (b) 0.2 g Mg variation, and (c) 0.1 g Mg variation

3.3. Characterization of Al6061/Sea Sand Composites

3.3.1. Density and porosity

The density values of the Al6061/sea sand composite are presented in Fig. 7. It was observed that an increase in the Mg content leads to a decrease in the density of the composite. Specifically, the density of the composite with additions of 0.1 g, 0.2 g, and 0.3 g of Mg was lower than that of the pure aluminum matrix $\left(2.7\ \mathrm{g/cm^3}\right)$. The measured densities of the composites were 2.643 $\mathrm{g/cm^3}$ for 0.1 g of Mg, 2.608 $\mathrm{g/cm^3}$ for 0.2 g of Mg, and 2.560 $\mathrm{g/cm^3}$ for 0.3 g of Mg.

The results of the porosity test for the composites containing 0.1 g, 0.2 g, and 0.3 g of Mg showed average porosities of 1.84%, 2.49%, and 3.34%, respectively (see Fig. 8). There is a linear relationship between increases in Mg content and porosity, but the porosity of the Al6061/Sea sand composite shows an inverse relationship with the increase in Mg content. The rise in porosity occurs because the Al 6061 matrix does not fully penetrate the sea sand particles during the fusion process. Specifically, there is a mismatch between the Mg content and the wet sand particles, which prevents the molten aluminum from adequately infiltrating the uncoated sea sand. Consequently, cracks form around the sea sand particles during the machining process, leading to porosity defects.

3.3.2. Microstructure

Figure 9 displays the findings from the microstructure characterization (zoom in 100 μ m). The data presented in the figure indicate that adding 0.1 g of Mg to the sea sand results in lower porosity than adding 0.2 g, which leads to higher porosity. Additionally, as shown in Fig. 9c, the porosity observed after adding 0.3 g of magnesium appears to be even greater.

The microstructure of the Al6061/sea sand composite is presented in Fig. 8. This figure shows that porosity increases linearly with increasing Mg content. This tendency is supported by the rougher surface of sea sand, which provides greater surface contact between the reinforcement and the matrix. These findings are in reasonable confor-

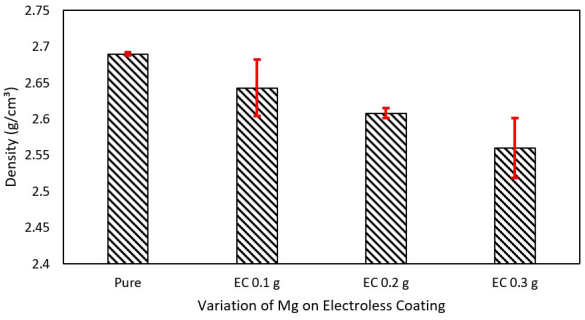

Fig. 7. The density of an Al6061-sea-sand composite with varying amounts of magnesium at electroless coating

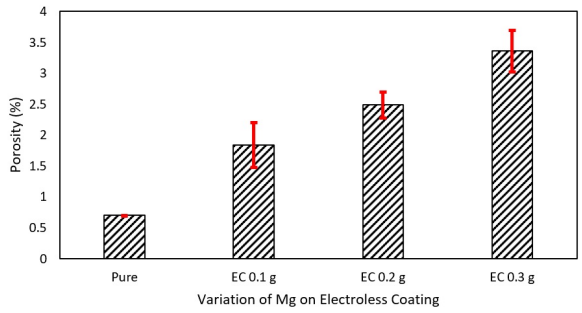

Fig. 8. The porosity value of composite Al6061/sea sand with varying Mg under electroless coating

mity with the previous research [17]. During composite manufacturing, another factor may contributing to porosity is the entrapment of gas during the pouring of the molten matrix into the mold. These trapped gases further increase the porosity of the composite. Microstructural observations indicate that the lowest porosity is achieved during the electroless coating process with 0.1% of Al. Conversely, porosity tends to increase with higher magnesium content in the electroless coating process. This illustrates a clear correlation between porosity and rising magnesium levels during the electroless coating process.

The lower porosity of the Al6061/Sea sand composite suggests the possibility of a higher hardness. This relation showed that the amount of Mg used during electroless coating significantly affects composite properties. Beyond its impact on porosity, Mg content also influences the dispersal of molten aluminum among sea sand particles, which subsequently affects the particle distribution within the composite. A more uniform particle distribution leads to improved mechanical properties of the composite. This enhancement is attributed to the Orowan strengthening mechanism, which impedes dislocation motion within the composite. The present study findings have a good conformity with the previous research of Akbar et al. [5] which the mechanical behaviour of sample has decreased linearly with the increase in porosity structure, and thats all is supported by the microstructure test.

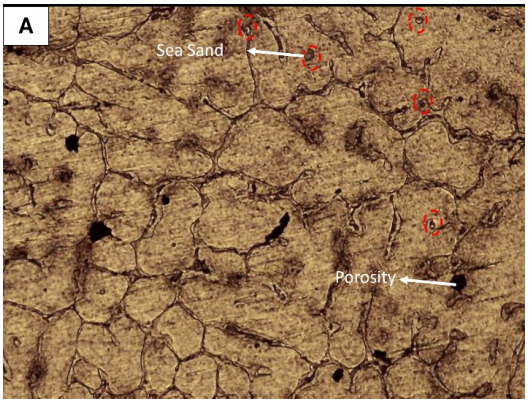

(a) 0.1 g

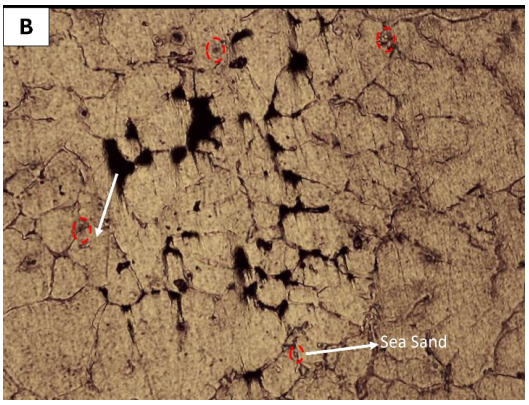

(b) 0.2 g

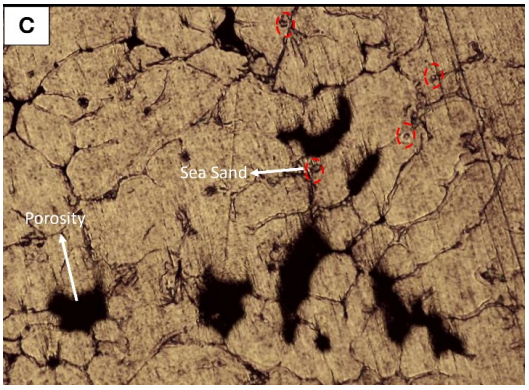

(c) 0.3 g

Fig. 9. The microstructure of an electroless coated A16061-coast sand composite with variation of magnesium

3.3.3. Hardness

As stated in the previous section, the increase in porosity is due to the rising Mg content. Therefore, a hardness test was conducted to reveal the relationship between the two

variables (porosity and Mg content) and the hardness value. Fig. 10 presents the hardness value of the Al6061/Sea sand composite.

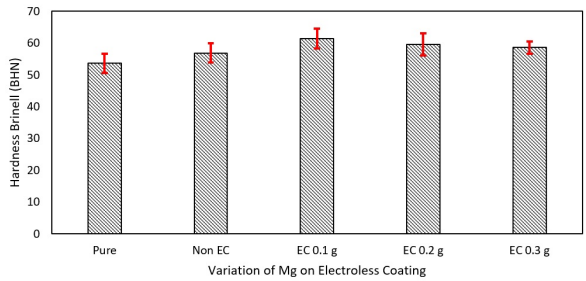

Fig. 10. The hardness value of composite Al6061/Sea sand

Fig. 10 shows that pure Al6061 has a lower hardness than the composite Al6061/Sea sand without an electroless coating, with hardness values of 53.6 BHN for pure Al6061 and 56.9 BHN for the composite, indicating a 6.15% increase in hardness. The electroless coating process also increases the hardness of the composite, with values of 61.5BHN, 59.6BHN, and 58.6 BHN for 0.1 g Mg, 0.2 g Mg, and 0.3 g Mg, respectively. According to this data, the increment value is 8.08% for 0.1 g Mg, 4.74 % for 0.2 g Mg, and 2.98% for 0.2 g Mg. This indicates that adding reinforcement to the composite effectively increases its hardness. Furthermore, using sea sand as a reinforcement is an effective way to enhance the composite's strength. The improvement in hardness can be attributed to the incorporation of sea sand, which serves to strengthen the aluminum matrix. Research has shown that the electroless coating process creates a spinel phase on the surface of sea sand particles. This spinel phase increases the particles' surface area, thereby enhancing the bond between the matrix and the reinforcing particles. The strong bond of the interface means the wettability of reinforcement and matrix increases, leading to improved mechanical strength [18].

The increase in Mg via electroless coating is proven to increase the composite's hardness compared to the composite without electroless coating. Specifically, the composite's hardness decreases linearly with increasing Mg content. The decreases in hardness from 0.1 g Mg are 3.18% for 0.2 g Mg and 4.945% for 0.3 g Mg. This shows that Mg content affects the distribution of reinforcing particles in the aluminum matrix as it increases. This result is because the composite with 0.2 g and 0.3 g Mg has a larger structural porosity than the 0.1 g Mg composite. According to the literature, clumps and hole formation in the structural material have significantly influenced the mechanical properties [19].

4. Conclusion

The experiment on using sea sand as a reinforcement material in a metal matrix composite has been successfully conducted. This research demonstrates that coating sea sand particles through an electroless coating process enhances the mechanical properties of the composite. Specifically, increasing the Mg content in the coating agent improves the mechanical properties compared to the uncoated version. However, a pore microstructure forms when the Mg concentration remains high, thereby reducing mechanical properties. These results indicate that both electroless coating and Mg content significantly influence the material's mechanical properties. Additionally, research on metal matrix composites has a vast potential for development, particularly with reinforcements derived from other waste materials such as fly ash, steel scrap, waste glass, and natural resources like coconut husks and rice husks.

References

[1] E. W. A. Fanani, E. Surojo, A. R. Prabowo, and H. I. Akbar, (2021) *"Recent progress in hybrid aluminum composite: Manufacturing and application"* **Metals *11***(12): 1919. DOI: 10.3390/met11121919.

[2] E. W. A. Fanani, E. Surojo, A. R. Prabowo, D. Ariawan, and H. I. Akbar, (2021) *"Recent development in aluminum matrix composite forging: Effect on the mechanical and physical properties"* **Procedia Structural Integrity *33***: 3–10. DOI: 10.1016/j.prostr.2021.10.002.

[3] S. Ravindran, N. Mani, S. Balaji, M. Abhijith, and K. Surendaran, (2019) *"Mechanical behaviour of aluminium hybrid metal matrix composites–a review"* **Materials Today: Proceedings *16***: 1020–1033. DOI: 10.1016/j.matpr.2019.05.191.

[4] K. K. Alaneme, B. O. Ademilua, and M. O. Bodunrin, (2013) *"Mechanical properties and corrosion behaviour of aluminium hybrid composites reinforced with silicon carbide and bamboo leaf ash"* **Tribology in Industry *35***(1): 25.

[5] H. I. Akbar, E. Surojo, D. Ariawan, and A. R. Prabowo, (2020) *"TECHNICAL INVESTIGATION OF SEA SAND REINFORCEMENT FOR NOVEL AL6061-SEA SAND COMPOSITES: IDENTIFICATION OF PERFORMANCE AND MECHANICAL PROPERTIES."* **Periódico Tchê Química *17***(36): DOI: 10.52571/PTQ.v17.n36.2020.63.

[6] S. Jannet, R. Raja, V. Arumugaprabu, G. V. Kumar, S. Vigneshwaran, P. R. Sreekanth, and K. Naresh, (2022) *"Effect of neem seed biochar on the mechanical and wear properties of aluminum metal matrix composites fabricated using stir casting"* **Materials Today: Proceedings *56***: 1507–1512. DOI: 10.1016/j.matpr.2021.12.572.

[7] P. Yadav, A. Ranjan, H. Kumar, A. Mishra, and J. Yoon, (2021) *"A contemporary review of aluminium MMC developed through stir-casting route"* **Materials *14***(21): 6386. DOI: 10.3390/ma14216386.

[8] L. Zhengwuvi, L. Timon, M. Hassan, and R. Joshua, (2023) *"Production and characterization of aluminium matrix composite with mixture of silicon carbide and groundnut shell ash as reinforcement for automotive application"* **Savannah Journal of Science and Engineering Technology *1***(5): 244–250.

[9] N. Panwar, M. Goud, S. Kant, et al., (2018) *"Experimental investigation of AA6061-Al2O3-fly ash composite produced by using stir casting method"* **Materials Today: Proceedings *5***(14): 28413–28419. DOI: 10.1016/j.matpr.2018.10.127.

[10] V. Chak, H. Chattopadhyay, and T. Dora, (2020) *"A review on fabrication methods, reinforcements and mechanical properties of aluminum matrix composites"* **Journal of manufacturing processes *56***: 1059–1074. DOI: 10.1016/j.jmapro.2020.05.042.

[11] B. C. Kandpal, H. Singh, et al., (2017) *"Fabrication and characterisation of Al2O3/aluminium alloy 6061 composites fabricated by Stir casting"* **Materials Today: Proceedings *4***(2): 2783–2792. DOI: 10.1016/j.matpr.2017.02.157.

[12] A. Zulfia and A. I. Adyatma, (2013) *"Electroless plating of Al2O3 particles reinforced composites"* **Advanced Materials Research *789***: 66–71. DOI: 10.4028/www.scientific.net/AMR.789.66DOIlink.

[13] A. Zulfia, (2010) *"Effect of Mg on formation of electroless plating on the surface of SiC particles reinforced composites"* **Journal of Materials Science and Engineering *4***(12): 12–17.

[14] A. I. Adityatama, (2010) *"The Effect of Magnesium on the Electroless Plating Process on Al2O3 Reinforcement Particles"* **Universitas Indonesia**:

[15] V. M. Sreekumar, R. M. Pillai, B. C. Pai, and M. Chakraborty, (2008) *"Microstructural development in Al/MgAl2O4 in situ metal matrix composite using value-added silica sources"* **Science and Technology of Advanced Materials**: DOI: 10.1088/1468-6996/9/1/015004.

[16] V. Sreekumar, N. H. Babu, D. Eskin, and Z. Fan, (2015) *"Structure–property analysis of in-situ Al–MgAl2O4 metal matrix composites synthesized using ultrasonic cavitation"* **Materials Science and Engineering: A *628***: 30–40. DOI: 10.1016/j.msea.2015.01.029.

[17] P. Garg, A. Jamwal, D. Kumar, K. K. Sadasivuni, C. M. Hussain, and P. Gupta, (2019) *"Advance research progresses in aluminium matrix composites: manufacturing & applications"* **Journal of materials research and technology *8***(5): 4924–4939. DOI: 10.1016/j.jmrt.2019.06.028.

[18] H. I. Akbar, E. Surojo, and D. Ariawan. "Effect of Sea Sand Content on Hardness of Novel Aluminium Metal Matrix Composite AA6061/Sea Sand". In: *Proceedings of the 6th International Conference and Exhibition on Sustainable Energy and Advanced Materials: ICE-SEAM 2019, 16—17 October 2019, Surakarta, Indonesia*. Springer. 2020, 307–315. DOI: 10.1007/978-981-15-4481-1_31.

[19] L. Yolshina and A. Kvashinchev, (2016) *"Chemical interaction of liquid aluminum with metal oxides in molten salts"* **Materials & Design *105***: 124–132. DOI: 10.1016/j.matdes.2016.05.012.